

# Coastal flood risk to European surface transport infrastructure at different global warming levels

Received: 10 June 2025

Accepted: 4 November 2025

Published online: 14 January 2026

 Check for updates

Khin Nawarat <sup>1,2</sup>✉, Johan Reynolds <sup>1,3,4</sup>, Michalis I. Vousdoukas <sup>5</sup>,  
Eamonn Mulholland <sup>6</sup>, Kees van Ginkel <sup>3,7</sup>, Luc Feyen <sup>8</sup>✉ &  
Roshanka Ranasinghe <sup>1,2,3</sup>

European coastal regions host a dense transport network that supports various human activities and well-being. However, global warming is expected to increase coastal flooding risk, whose impact on existing and planned European transport systems remains unknown. Here we present the fully probabilistic assessment of coastal flood risk to Europe's surface transport infrastructure at different levels of global warming. Under baseline conditions (1980–2020), we find 1,592 km of networks are affected annually, causing expected annual damage of up to €722 million. Roads are projected to be more affected than railways in all countries. Passenger and haulage transport within the low-elevation coastal zone are currently overwhelmingly road dependent, which signals potential for widespread disruptions unless transportation modes change. With 1.5 °C warming, the Europe-wide expected annual damage may reach €1,108 million, and with 4 °C, it is projected to be as high as €1,487 million. Adaptation expenditures will increase with every fraction of global warming in most countries.

The coastal zone is characterized by high population densities and the presence of transport, cultural and economic infrastructure. In the European Union, approximately one-third of the population resides within 50 km of the coast<sup>1</sup>. The Sixth Assessment Report of the Intergovernmental Panel on Climate Change (IPCC AR6) states with high confidence that extreme sea level events, which can lead to coastal flooding, will become more intense and frequent over the twenty-first century in almost all regions of the world<sup>2,3</sup>. Previous studies have projected that without adequate mitigation and adaptation measures, coastal flooding along the European coastline could result in expected annual damage (EAD) of up to €240 billion by 2100 under the high-emission Representative Concentration Pathway (RCP8.5)<sup>1</sup>, a more than 170-fold increase over the present-day EAD of €1.4 billion.

Transport infrastructure is particularly important among civil infrastructure due to its pivotal role in mobility, trade and

communication<sup>4–10</sup>. With increasing urbanization and maritime activity, transport infrastructure has become more concentrated in the European coastal areas<sup>11</sup>. The European Union is working towards completing the Trans-European Transport (TEN-T) core network by 2030 and a more extended, comprehensive transport network by 2050, prioritizing the development and interconnection of major transport corridors<sup>12</sup>. Many of these planned investments are located in coastal regions to enhance cross-border mobility and economic integration. At the same time, these coastal areas are at increasing risk from coastal flooding due to global warming, highlighting the importance of aligning infrastructure planning with climate resilience.

Despite the urgency for large-scale risk information, most coastal flood-risk assessments remain focused on regional scales<sup>13–16</sup>. Although European-scale projections of coastal flood risk do exist, they generally do not address impacts on transport infrastructure specifically,

<sup>1</sup>IHE Delft Institute for Water Education, Delft, The Netherlands. <sup>2</sup>University of Twente, Enschede, The Netherlands. <sup>3</sup>Deltares, Delft, The Netherlands.

<sup>4</sup>Delft University of Technology, Delft, The Netherlands. <sup>5</sup>Department of Marine Sciences, University of Aegean, Mytilene, Greece. <sup>6</sup>Department for Transport, London, UK. <sup>7</sup>Institute for Environmental Studies (IVM), Vrije Universiteit, Amsterdam, The Netherlands. <sup>8</sup>Joint Research Centre, Ispra, Italy.

✉e-mail: [k.nawarat@un-ihe.org](mailto:k.nawarat@un-ihe.org); [Luc.FEYEN@ec.europa.eu](mailto:Luc.FEYEN@ec.europa.eu)

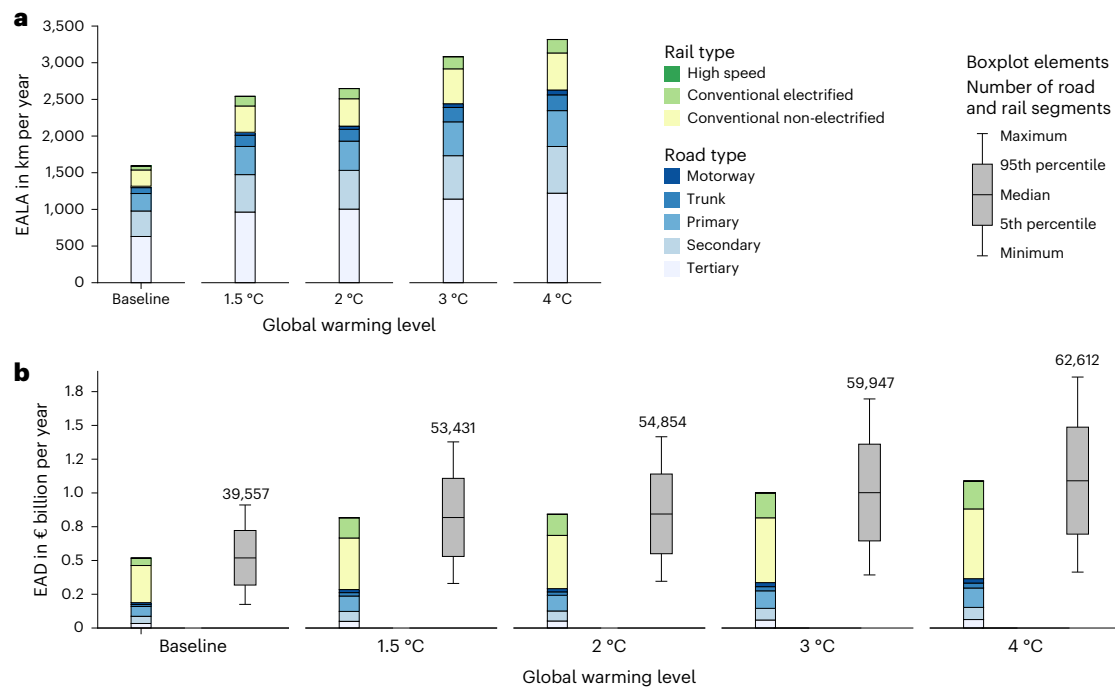


**Fig. 1 | Coastal flood risk to surface transport infrastructure in Europe by transport type for different global warming levels. a, EALA. b, Median EAD (colour bar plot) and the associated uncertainty range of it. The grey box plots show the 5th percentile, median and 95th percentile values, with whiskers extending to the minimum and maximum values. The EAD distributions were**

derived from probabilistic EAD estimates for individual road and rail segments (1,000 EAD samples per segment). The number of segments for each distribution is shown above each boxplot. Baseline values are for 1980–2020 climate conditions.

focusing instead on general exposure metrics such as population, gross domestic product (GDP) or sectoral damages<sup>17–19</sup>. There are a few global-scale studies that project future coastal flood risks under climate change scenarios, but these largely emphasize population and socio-economic exposure<sup>20–25</sup>. On transport infrastructure specifically, existing large-scale flood-risk assessments have primarily concentrated on fluvial flooding, with studies assessing impacts on roads<sup>26–28</sup> and railways separately across Europe<sup>29</sup>. However, detailed assessments of coastal flood risk to European transport infrastructure, including both road and rail networks, under present and future global warming levels are lacking in the scientific literature to date.

The very few previous studies that have specifically focused on fluvial flood damage to transport infrastructure show that flooding of road and rail networks comprises a large share of all direct tangible flood losses, typically ranging from 5% to 10% and up to 50% to 60% of the total flood damage in cases where the exposed network is extensive—for example, in highly urbanized or infrastructure-dense regions<sup>30</sup>. However, these studies provide only approximate estimations, employing broad assumptions, such as using gridded land-cover maps to determine exposed transport networks, applying a single damage function and assuming a uniform maximum damage value for all types of transport infrastructure. One reason for the lack of detailed flood damage modelling for transport infrastructure is that narrow, line-like transport networks are difficult to capture with the low-resolution gridded land-cover maps commonly used in flood impact/risk studies<sup>27,29,31,32</sup>.

Another challenge in quantifying the damage to transport infrastructure relates to vulnerability evaluation. In flood-risk studies, vulnerability is often translated into a damage value by multiplying the fractional damage associated with a given flood depth (typically derived from depth-damage (DD) curves), with the reconstruction cost of the asset<sup>27,29,31,32</sup>. Defining these DD curves and assessing reconstruction costs at a large scale is particularly challenging due to the diversity of road and rail types, their varying damage for different flood depths

and widely varying construction practices and costs across different countries<sup>33</sup>. Consequently, large-scale impact assessments inevitably rely on broad generalizations to account for these variations in vulnerability input data<sup>32</sup>. Thus, the lack of high-resolution datasets with relevant attributes, type-specific damage data and computational resource limitations have been a substantial barrier to conduct detailed large-scale flood-risk assessments of transport infrastructure.

Recently, the OpenStreetMap (OSM) dataset, which is feature-based and almost complete for most European countries<sup>34</sup>, has enabled more accurate large-scale damage estimates. Building on this, the model GMTRA was introduced for global-scale multi-hazard risk analysis, estimating the multi-hazard-related annual damage of transport networks, but only for the current climatic conditions, by treating road and rail segments as line objects with attributes<sup>32</sup>. This approach has since been applied in continental-scale fluvial flood-risk assessments of European road infrastructure for current climate conditions<sup>27,28</sup> and for rail infrastructure under different global warming levels<sup>29</sup>, with improvements in DD curves and reconstruction costs. However, to date, a comprehensive assessment of coastal flood risk to surface transport infrastructure, including both road and rail networks, at a European scale has not been attempted, the knowledge gaps this study is specifically designed to address.

Here we assess the coastal flood risk to European road and rail networks across a range of global warming levels. We present projections for global mean temperature rises of 1.5 °C and 2 °C (relative to 1850–1900), aligned with the Paris Agreement temperature targets and higher global warming levels of 3 °C and 4 °C (relative to 1850–1900). We integrate coastal flood maps (derived from process-based numerical modelling) for the aforementioned global warming levels, existing road and rail networks together with their attributes and type-specific flood depth-related reconstruction costs to calculate total damage. Risk is reported probabilistically in terms of EAD in euros per year, which represents the average annual damage from all possible coastal flood events, accounting for both the

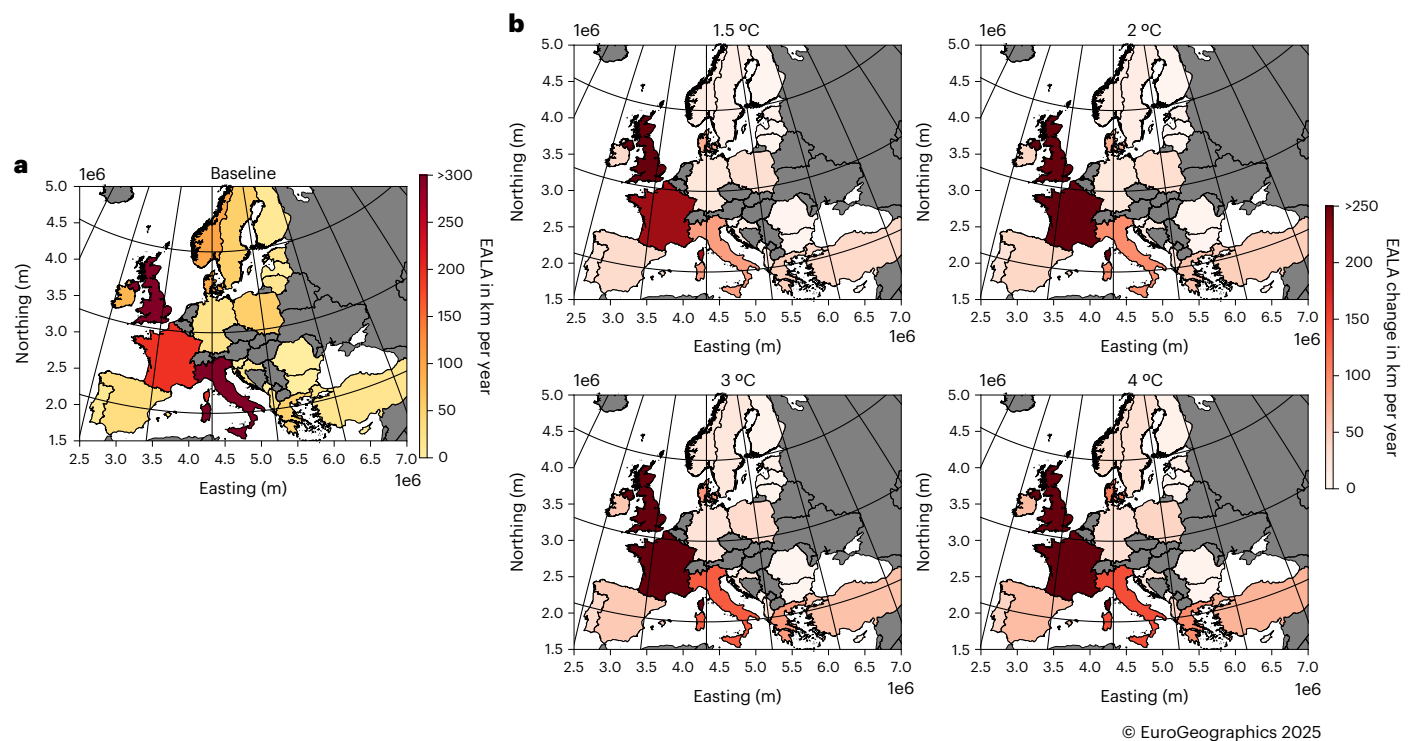


**Fig. 2 | Coastal flood risk to surface transport infrastructure in Europe expressed as EALA for different global warming levels at the country scale.** **a**, Baseline EALA (the estimate under 1980–2020 climate conditions). **b**, The change in EALA from the baseline value for different global warming levels; the

Netherlands and Belgium are not affected by the range of flood-return periods considered in this study due to the very high levels of coastal protection already in place. Basemap administrative boundaries from EuroGeographics 2025 under a licence available at <https://www.mapsforeurope.org/licence>.

probability of each event and the damage it would cause. We also calculate the expected annual length (of roads and railways) affected (EALA) in kilometres per year, reflecting the average annual extent of surface transport infrastructure affected by coastal flooding. These metrics are provided at national and continental levels (results at the Nomenclature of Territorial Units for Statistics, level 3 (NUTS3) region and IPCC AR6 subregion levels are also given in Supplementary Figs. 1 and 2 and Supplementary Tables 1 and 2; for ease of reference, a summary table highlighting the key findings from our analysis is included as Supplementary Table 3).

### European-scale assessment

We find that 1,592 km of road and rail networks are annually affected by coastal flood events under baseline (1980–2020) climate conditions (Fig. 1a). As the global mean temperature rises, this amount is projected to increase substantially. For a global warming level of 1.5 °C relative to 1850–1900, the projected EALA increases to 2,542 km, an ~60% increase from the baseline. At 2, 3 and 4 °C of warming, the EALA increases further to 2,648 km (66% more than the baseline value), 3,083 km (93% more than the baseline value) and 3,317 km (108% more than the baseline value), respectively.

Looking further into the exposure and risk faced by different types of surface transport infrastructure in Europe, road networks emerge as being more affected by coastal flooding than railways (Fig. 1a). This is probably because most European countries have a greater extent of roads than railways within the low-elevation coastal zone (LECZ), defined as areas  $\leq 10$  m above mean sea level<sup>35,36</sup>, making them more exposed to coastal flooding (Supplementary Table 4). Considering baseline EALAs, tertiary roads account for the largest share of total EALA, with 630 km, representing 40% of the total. Secondary roads follow with 348 km affected (22% of the total EALA), followed by primary roads (238 km, or 15% of the total EALA) and conventional non-electrified rails (222 km, or 14% of the total EALA).

The above annually affected lengths are directly associated with economic damage, which is here quantified in terms of the EAD (Fig. 1b). Our assessment indicates a baseline (1980–2020) EAD of approximately €519 million [€318 million–€722 million] (median [5th–95th percentiles]) for Europe. With 1.5 °C of global warming, the EAD is projected to increase to €818 million [€530 million–€1,108 million]: an increase of about 58% from the baseline EAD. With 2 °C of warming, the EAD is projected to increase to €844 million [€550 million–€1,140 million], reflecting a 62% increase from the baseline value. The projected EAD values increase even further with 3 °C of warming, with the median EAD increasing to €1,002 million [€645 million–€1,361 million] (a 93% increase from the baseline). Should the global warming level reach 4 °C, the EAD is projected to rise as high as €1,090 million [€695 million–€1,487 million], more than doubling the median baseline EAD.

In contrast to the predominant affected length of road networks over railways in total EALA, rail damage comprises a larger portion of the total EAD. This is probably because reconstruction of rail infrastructure is generally more expensive than that of roads<sup>37</sup>. Specifically, the EAD related to conventional non-electrified rails for the baseline is €275 million, which accounts for half of the total EAD (Fig. 1b). This dominance of the European-scale EAD by rail infrastructure compared to that associated with roads increases with higher levels of global warming (Fig. 1b).

### Country-level assessment

The largest EALA for baseline conditions is in Italy (436 km), UK (355 km), France (195 km), Norway (100 km) and Denmark (not including Greenland) (94 km) (Fig. 2a). All of these countries are projected to experience a substantial increase in their EALA with increasing global warming levels. Even under the lowest-considered global warming level of 1.5 °C, the projected increases in EALA from baseline values are substantial, with increases of 19% in Italy, 77% in UK, 114% in France, 12% in Norway and 77% in Denmark (Fig. 2b).

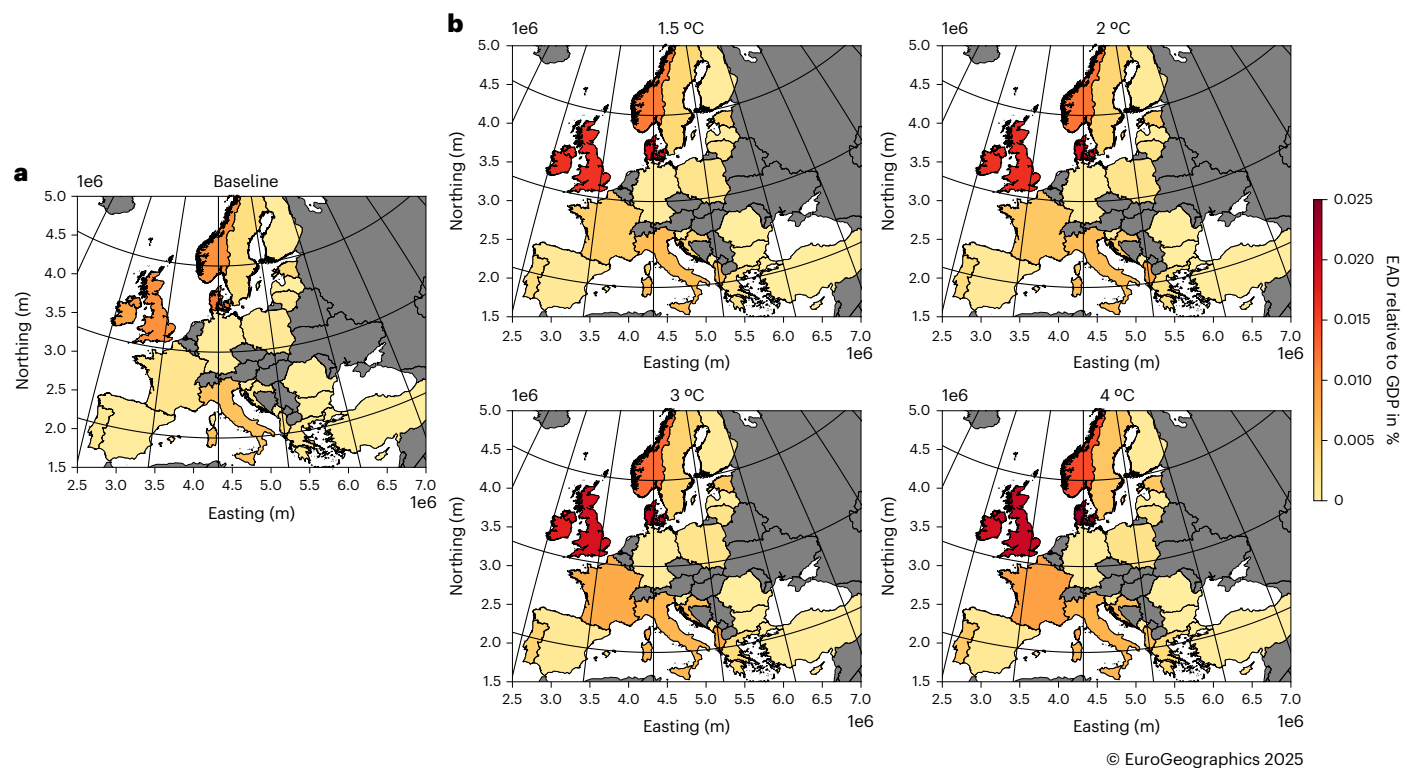


**Fig. 3 | Coastal flood risk to surface transport infrastructure in Europe expressed as EAD relative to national GDP for different global warming levels at the country scale. a**, EAD expressed as a percentage of national GDP for the baseline (the estimate under 1980–2020 climate conditions). **b**, EAD expressed as a percentage of national GDP for different global warming levels (assuming no

change in future GDP) (data from ref. 42); the Netherlands and Belgium are not affected by the range of flood-return periods considered in this study due to the very high levels of coastal protection already in place. Basemap administrative boundaries from EuroGeographics 2025 under a licence available at <https://www.mapsforeurope.org/licence>.

Interestingly, the higher EALA in these countries appears not to be primarily linked to the extent of LECZ. For example, UK's EALA for baseline conditions (355 km) is much higher than that of France (195 km). However, UK and France have more or less the same LECZ areas per kilometre of coastline length ( $1.34 \text{ km}^2 \text{ km}^{-1}$  and  $1.35 \text{ km}^2 \text{ km}^{-1}$ , respectively) (Supplementary Table 5<sup>38–40</sup>). In Norway, the LECZ area per kilometre of coastline is rather low ( $0.25 \text{ km}^2 \text{ km}^{-1}$ ), yet Norway ranks among the top-five countries in terms of EALA (baseline conditions). To further investigate the current exposure (that is, baseline conditions) of surface transport networks to coastal flooding in each European country, we calculated the percentage of the national transport network located in the LECZ of each country (Supplementary Table 4). This analysis reveals that UK has a higher percentage of its national transport network in the LECZ (8%) than France (3%). Norway has 8.1% of its national transport network situated in the LECZ, ranking sixth among the coastal countries in Europe where this statistic is concerned. It must be noted that, while in the above analysis we focused only on the LECZ area and the current exposure as key factors that may elevate the EALA in a given country, other aspects, such as storm characteristics and the overall extent of transport networks, could also play a role in elevating (or diminishing) EALA.

The passenger and haulage transport activities<sup>41</sup> in the LECZ are also higher in the aforementioned top-five EALA countries compared to other European countries (with the exceptions of Netherlands, Germany and Belgium) (Extended Data Fig. 1a,c). This is particularly concerning with respect to possible socio-economic impacts and supply-chain disruption during coastal flood events.

Under baseline conditions, coastal flooding affects more roads than railways in all European countries except Latvia and Slovenia (stacked bars in Extended Data Fig. 2a provide baseline-condition values). With global warming (for all warming levels considered here),

even these two exceptions disappear, and roads are projected to be more exposed to coastal flooding than railways in every European country, across all considered global warming levels (example of 2 °C of warming in Extended Data Fig. 2a). It is therefore a great concern that passenger and haulage transport activities within the LECZ predominantly rely on road networks rather than rail networks in a vast majority of European countries (Extended Data Fig. 1b,d), meaning that transport disruptions due to coastal flooding and associated direct and indirect socio-economic impacts are likely to be severe (unless road and rail networks, and their relative usage, change drastically through the twenty-first century from what they are at present).

In terms of the financial risk associated with the surface transport network affected by coastal flooding, under baseline conditions, the UK has the highest EAD (Extended Data Fig. 3a), totalling €272 million, which is more than half of the total European baseline EAD. Italy has the second-highest EAD, with €93 million, followed by Norway, France and Denmark, with EADs of €35 million, €34 million and €33 million, respectively. (Note: Cyprus and Malta do not have the rail types we considered in this study.)

Our projections show that EAD increases with global warming for every European country (Extended Data Fig. 3b). Cyprus, Bulgaria, France, Croatia and Romania are projected to experience the largest increase in EAD compared to other European countries (relative to baseline-condition EADs). Even at the lowest global warming level considered (1.5 °C), EAD is expected to rise substantially in these countries—Cyprus stands out with a tenfold increase relative to its baseline EAD, followed by Bulgaria, France, Croatia and Romania, each with an approximately threefold increase. Among all countries, Cyprus emerges as the most sensitive to global-warming-induced coastal flood impacts. Although the EAD values in Cyprus are not among the highest (Extended Data Fig. 3a), the rate of increase

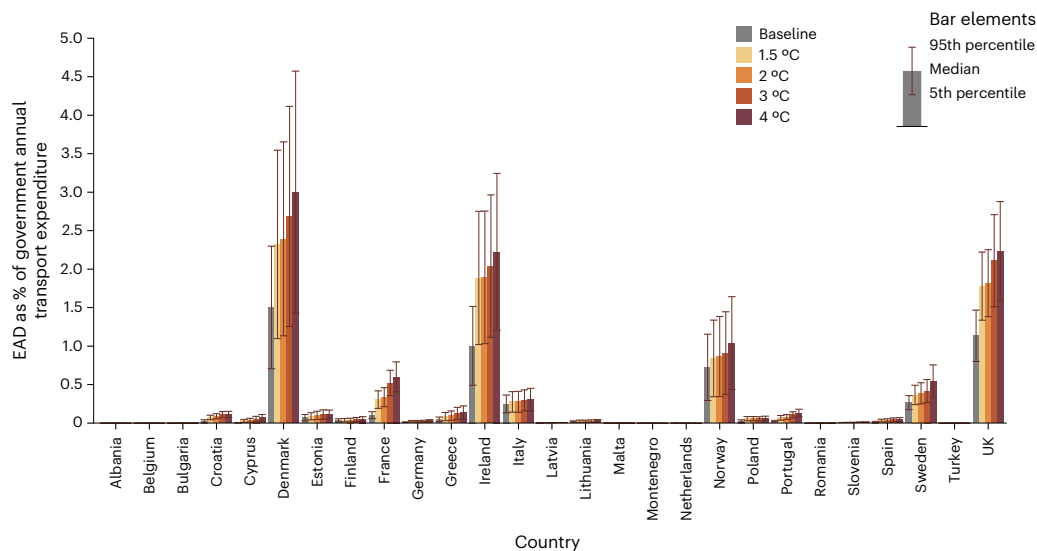


**Fig. 4 | Coastal flood risk to surface transport infrastructure in Europe expressed as EAD relative to annual government expenditures on road and rail networks for baseline conditions and for different global warming levels.** Bars represent the median (50th percentile) of aggregated country-level EAD distributions, and error bars indicate the 5th–95th percentile ranges. Each national EAD distribution was derived from probabilistic EAD estimates for individual road and rail segments (1,000 EAD samples per segment), aggregated to the country level. The number of segments per country under baseline–4 °C is as follows: Bulgaria 25–37, Croatia 456–666, Cyprus 86–159, Germany 862–1,365, Denmark 2,053–3,210, Estonia 282–362, Finland 597–728, France

7,791–14,529, Greece 910–1,808, Ireland 1,949–2,554, Italy 4,164–6,636, Latvia 80–235, Lithuania 88–125, Norway 2,595–3,125, Poland 936–1,469, Portugal 1,007–1,436, Romania 38–66, Spain 1,656–2,841, Sweden 1,686–2,468, Slovenia 138–262 and United Kingdom 11,374–16,810. Annual government expenditures on road and rail infrastructure estimates used here include investment, operation and maintenance costs for 2016, adjusted to 2015 price levels in euros. Albania, Montenegro and Turkey could not be considered in this analysis due to unavailability of data. (Data from ref. 43). The Netherlands and Belgium are not affected by the range of flood-return periods considered in this study due to their already very high levels of coastal protection.

7,791–14,529, Greece 910–1,808, Ireland 1,949–2,554, Italy 4,164–6,636, Latvia 80–235, Lithuania 88–125, Norway 2,595–3,125, Poland 936–1,469, Portugal 1,007–1,436, Romania 38–66, Spain 1,656–2,841, Sweden 1,686–2,468, Slovenia 138–262 and United Kingdom 11,374–16,810. Annual government expenditures on road and rail infrastructure estimates used here include investment, operation and maintenance costs for 2016, adjusted to 2015 price levels in euros. Albania, Montenegro and Turkey could not be considered in this analysis due to unavailability of data. (Data from ref. 43). The Netherlands and Belgium are not affected by the range of flood-return periods considered in this study due to their already very high levels of coastal protection.

is striking: a tenfold increase at 1.5 °C, a 12-fold increase at 2 °C, an 18-fold increase at 3 °C and a 23-fold increase at 4 °C of global warming (Extended Data Fig. 3b).

We also present the EAD of each country (for baseline conditions and all considered warming levels) as a percentage of national GDP<sup>42</sup> (Fig. 3). Under baseline conditions, the countries with the highest EADs relative to their GDP are, in descending order, Denmark, UK (which nevertheless has the highest EAD, by far), Norway, Ireland and Italy. It is noteworthy, that countries with lower EADs, such as Estonia and Albania (only €0.7 million and €0.2 million, respectively; Extended Data Fig. 3a), are at a higher relative economic impact compared to, for example, France, which has a much higher EAD of €34 million. This illustrates that the economic impact of coastal flooding can be disproportionately severe for countries with smaller economies, even if their EAD figures themselves are lower. The EAD relative to GDP is projected to increase with the warming level in all European countries (Fig. 3), highlighting that every fraction of warming has economic consequences across Europe in terms of coastal flood damage to surface transport networks.

### Realignment of national surface transport expenditures

If the risk of coastal-flooding-induced damage to surface transport networks increases, governments will inevitably need to allocate more funds to maintain these important assets. To investigate how this may play out over the twenty-first century, we compared our EAD values to government annual expenditures on road and rail infrastructure<sup>43</sup> (Fig. 4; government annual expenditures on road and rail infrastructure for each European country are shown in Supplementary Table 6). Specifically, we examined how current and future EAD might force countries to reconsider their annual total transport budgets and how these budgets may need to be distributed between road and rail networks. Our results show that among European nations, the percentage increase in expenditure that might be required to counter coastal-flooding-induced damage to surface transport

networks as global mean temperature increases is highest in Denmark, Ireland and the UK. For example, the median baseline-condition EAD in Denmark now comprises 1.5% of its total annual surface transport expenditure. This share is projected to increase to 2.3% even under the lowest-considered global warming of 1.5 °C, meaning the country would need to increase its total annual surface transport expenditure (median estimate) by an additional €18 million at this global warming level. In Ireland and the UK, the median additional annual expenditures that would be required for the same warming level are €20 million and €155 million, respectively. For the highest-considered global warming level of 4 °C, median additional annual expenditures in Denmark, Ireland and the UK are as high as €33 million, €28 million and €263 million.

For the other two countries that were among the top five in terms of EAD relative to GDP, Italy and Norway, the additional investment required for surface transport infrastructure is comparatively modest. Under the lowest warming scenario of 1.5 °C, the median additional annual expenditures are projected to be €10 million for Italy and €5 million for Norway. Under the highest-considered warming scenario of 4 °C, these figures increase to €20 million and €15 million, respectively.

Our results indicate not only the potential need to allocate a larger share of the national transport expenditure to counter coastal flood risk to surface transport networks but also that transport investment priorities may need to shift from roads to railways in the LECZ, or vice versa, depending on the transport infrastructure type most affected by coastal flooding in a given country. For instance, in Croatia, road damage currently contributes more than rail damage to the total EAD (Extended Data Fig. 2b). Correspondingly, the government's annual transport expenditure within the LECZ is tilted towards roads (Extended Data Fig. 1f). However, for 2 °C of global warming, damage to rail infrastructure in Croatia is projected to surpass that of roads (Extended Data Fig. 2b). This shift would necessitate a realignment of Croatia's transport expenditure within the LECZ, with more

resource allocation for rail infrastructure than for roads (assuming the total surface transport infrastructure remains much the same). Unless the total available budget increases adequately, such a realignment of resources would necessitate a reduction in government expenditure for roads, which could present new challenges as passenger and haulage transport in Croatia's LECZ predominantly relies on road networks (Extended Data Fig. 1b,d). In contrast, in Bulgaria, rail damage currently accounts for a larger share of the total baseline-condition EAD (Extended Data Fig. 2b), and consequently, current transport expenditure is slightly tilted towards rail infrastructure (Extended Data Fig. 1f). However, our projections indicate that for a 2 °C global warming level, coastal-flooding-induced road damage will become larger than rail damage, potentially requiring a shift in expenditure priorities towards roads. This could constrain resources available for rail networks, despite rail being the primary mode of haulage transport in Bulgaria (Extended Data Fig. 1d), unless the total available budget increases sufficiently. Our results point towards the potential need for such a realignment of transport resource allocation in France as well.

In addition to these findings, climate change adaptation in the transport sector remains inadequate in many regions of Europe<sup>44</sup>. Our EAD projections are based on current infrastructure and static exposure, effectively representing a no-adaptation scenario. If adaptation investments continue to lag, the economic losses projected here are likely to materialize. Furthermore, actual future impacts could exceed these estimates if exposure increases—for example, due to continued development of transport infrastructure, particularly climate-vulnerable infrastructure, in LECZs. These findings highlight the urgent need for increased investment in climate-resilient infrastructure, especially in countries where the relative economic impact is projected to be high. Beyond economic implications, disruptions to transport infrastructure may also adversely affect social well-being and stability, particularly by limiting access to essential services, isolating vulnerable communities and reducing overall societal resilience to climate impacts<sup>44</sup>.

## Online content

Any methods, additional references, Nature Portfolio reporting summaries, source data, extended data, supplementary information, acknowledgements, peer review information; details of author contributions and competing interests; and statements of data and code availability are available at <https://doi.org/10.1038/s41558-025-02510-y>.

## References

- Feyen, L., Gosling, S., Ibarreta, D., Soria, A. & Ciscar, J. C. *Climate Change Impacts and Adaptation in Europe* (Publications Office of the European Union, 2020); <https://doi.org/10.2760/171121>
- Fox-Kemper, B. et al. in *Climate Change 2021: The Physical Science Basis* (eds Masson-Delmotte, V. et al.) 1211–1362 (Cambridge Univ. Press, 2023); <https://doi.org/10.1017/9781009157896.011>
- Ranasinghe, R. et al. in *Climate Change 2021: The Physical Science Basis* (eds Masson-Delmotte, V. et al.) 1767–1926 (Cambridge Univ. Press, 2021); <https://doi.org/10.1017/9781009157896.014>
- Council Directive 2008/114/EC of 8 December 2008 on the Identification and Designation of European Critical Infrastructures and the Assessment of the Need to Improve their Protection (Council of the European Union, 2008).
- Presidential Policy Directive—Critical Infrastructure Security and Resilience (Office of the Press Secretary, White House, 2013).
- Sendai Framework for Disaster Risk Reduction 2015–2030. A/CONF.224/CRP.1 (United Nations, 2015).
- Polyzos, S. & Tsiotas, D. The contribution of transport infrastructures to the economic and regional development: a review of the conceptual framework. *Theor. Empir. Res. Urban Manage.* **15**, 5–23 (2020).
- Nikolaou, P. & Basbas, S. Urban development and transportation: investigating spatial performance indicators of 12 European Union coastal regions. *Land* **12**, 1757 (2023).
- Yang, L. et al. Integrated design of transport infrastructure and public spaces considering human behavior: a review of state-of-the-art methods and tools. *Front. Archit. Res.* **8**, 429–453 (2019).
- Yu, P. et al. Nature-based solutions in coastal urbanization: addressing environmental and socio-economic challenges. Preprint at *Earth Critical Zone* <https://doi.org/10.1016/j.ecz.2025.100032> (2025).
- European Environment Agency *The Changing Faces of Europe's Coastal Areas* (Office for Official Publications of the European Communities, 2006).
- Trans-European Transport Network (TEN-T). *European Commission* [https://transport.ec.europa.eu/transport-themes/infrastructure-and-investment/trans-european-transport-network-ten-t\\_en](https://transport.ec.europa.eu/transport-themes/infrastructure-and-investment/trans-european-transport-network-ten-t_en) (2022).
- Silva, S. F. et al. An index-based method for coastal-flood risk assessment in low-lying areas (Costa de Caparica, Portugal). *Ocean Coast. Manage.* **144**, 90–104 (2017).
- Martinez-Graña, A. M., Boski, T., Goy, J. L., Zazo, C. & Dabrio, C. J. Coastal-flood risk management in central Algarve: vulnerability and flood risk indices (South Portugal). *Ecol. Indic.* **71**, 302–316 (2016).
- Armaroli, C. & Duo, E. Validation of the coastal storm risk assessment framework along the Emilia-Romagna coast. *Coastal Eng.* **134**, 159–167 (2018).
- Schlumberger, J. et al. Developing a framework for the assessment of current and future flood risk in Venice, Italy. *Nat. Hazards Earth Syst. Sci.* **22**, 2381–2400 (2022).
- Vousdoukas, M. I. et al. Economic motivation for raising coastal flood defenses in Europe. *Nat. Commun.* **11**, 2119 (2020).
- Vousdoukas, M. I. et al. Climatic and socioeconomic controls of future coastal flood risk in Europe. *Nat. Clim. Change* **8**, 776–780 (2018).
- Hinkel, J., Nicholls, R., Vafeidis, A., Tol, R. & Avagianou, T. Assessing risk of and adaptation to sea-level rise in the European Union: an application of DIVA. *Mitig. Adapt. Strateg. Glob. Chang.* **15**, 703–719 (2010).
- Kirezci, E. et al. Projections of global-scale extreme sea levels and resulting episodic coastal flooding over the 21st century. *Sci. Rep.* **10**, 11629 (2020).
- Kirezci, E., Young, I. R., Ranasinghe, R., Lincke, D. & Hinkel, J. Global-scale analysis of socioeconomic impacts of coastal flooding over the 21st century. *Front. Mar. Sci.* <https://doi.org/10.3389/fmars.2022.1024111> (2023).
- Mortensen, E. et al. The potential of global coastal flood risk reduction using various DRR measures. *Nat. Hazards Earth Syst. Sci.* **24**, 1381–1400 (2024).
- Jongman, B., Ward, P. J. & Aerts, J. C. J. H. Global exposure to river and coastal flooding: long term trends and changes. *Glob. Environ. Change* **22**, 823–835 (2012).
- Lloyd, S., Kovats, S., Chalabi, Z., Brown, S. & Nicholls, R. Modelling the influences of climate change-associated sea-level rise and socioeconomic development on future storm surge mortality. *Clim. Change* <https://doi.org/10.1007/s10584-015-1376-4> (2015).
- Neumann, B., Vafeidis, A. T., Zimmermann, J. & Nicholls, R. J. Future coastal population growth and exposure to sea-level rise and coastal flooding—a global assessment. *PLoS ONE* **10**, e0118571 (2015).
- Nemry, F. & Demirel, H. *Impacts of Climate Change on Transport: A Focus on Road and Rail Transport Infrastructures* (Publications Office of the European Union, 2012); <https://doi.org/10.2791/15504>

27. Van Ginkel, K. C. H., Dottori, F., Alfieri, L., Feyen, L. & Koks, E. E. Flood risk assessment of the European road network. *Nat. Hazards Earth Syst. Sci.* **21**, 1011–1027 (2021).
28. van Ginkel, K. C. H., Koks, E. E., de Groen, F., Nguyen, V. D. & Alfieri, L. Will river floods ‘tip’ European road networks? A robustness assessment. *Transp. Res. Part D: Transp. Environ.* **108**, 103332 (2022).
29. Bubeck, P. et al. Global warming to increase flood risk on European railways. *Clim. Change* **155**, 19–36 (2019).
30. Jongman, B. et al. Comparative flood damage model assessment: towards a European approach. *Nat. Hazards Earth Syst. Sci.* **12**, 3733–3752 (2012).
31. Kellermann, P., Schöbel, A., Kundela, G. & Thieken, A. H. Estimating flood damage to railway infrastructure—the case study of the March River flood in 2006 at the Austrian Northern Railway. *Nat. Hazards Earth Syst. Sci.* **15**, 2485–2496 (2015).
32. Koks, E. E. et al. A global multi-hazard risk analysis of road and railway infrastructure assets. *Nat. Commun.* **10**, 2677 (2019).
33. Nirandjan, S. et al. Review article: physical vulnerability database for critical infrastructure hazard risk assessments—a systematic review and data collection. *Nat. Hazards Earth Syst. Sci.* **24**, 4341–4368 (2024).
34. Barrington-Leigh, C. & Millard-Ball, A. The world’s user-generated road map is more than 80% complete. *PLoS ONE* **12**, e0180698 (2017).
35. McGranahan, G., Balk, D. & Anderson, B. The rising tide: assessing the risks of climate change and human settlements in low elevation coastal zones. *Environ. Urban.* **19**, 17–37 (2007).
36. Oppenheimer, M. et al. in *IPCC Special Report on the Ocean and Cryosphere in a Changing Climate* (eds Pörtner, H.-O. et al.) 321–445 (Cambridge Univ. Press, 2019).
37. *Round Table on Transport Economics, European Conference of Ministers of Transport Economic Research Centre, Transport Research Centre, Estimation and Evaluation of Transport Costs* (OECD, European Conference of Ministers of Transport, 2007).
38. Center for International Earth Science Information Network, Columbia University and CUNY Institute for Demographic Research, City University of New York *Low Elevation Coastal Zone (LECZ) Urban-Rural Population and Land Area Estimates* ver. 3 (NASA Socioeconomic Data and Applications Center, 2021); <https://doi.org/10.7927/d1x1-d702>
39. MacManus, K., Balk, D., Engin, H., McGranahan, G. & Inman, R. Estimating population and urban areas at risk of coastal hazards, 1990–2015: how data choices matter. *Earth Syst. Sci. Data* **13**, 5747–5801 (2021).
40. Coastal and marine ecosystems—marine jurisdictions: coastline length. *World Resources Institute* <https://web.archive.org/web/20120419075053/http://earthtrends.wri.org/text/coastal-marine/variable-61.html> (2024).
41. *EU Transport in Figures: Statistical Pocketbook 2024* (European Commission Directorate-General for Mobility and Transport, 2024); [https://transport.ec.europa.eu/facts-funding/studies-data/eu-transport-figures-statistical-pocketbook/statistical-pocketbook-2024\\_en](https://transport.ec.europa.eu/facts-funding/studies-data/eu-transport-figures-statistical-pocketbook/statistical-pocketbook-2024_en)
42. *Gross Domestic Product at Market Price in 2015* (Statistical Office of the European Union, European Commission, 2022); <https://doi.org/10.2908/TIPSAU10>
43. *Overview of Transport Infrastructure Expenditures and Costs* (European Commission Directorate-General for Mobility and Transport, 2019); <https://doi.org/10.2832/853267>
44. Dodman, D. et al. in *Climate Change 2022: Impacts, Adaptation and Vulnerability* (Pörtner, H.-O. et al.) 907–1040 (Cambridge Univ. Press, 2022); <https://doi.org/10.1017/9781009325844.008>

**Publisher’s note** Springer Nature remains neutral with regard to jurisdictional claims in published maps and institutional affiliations.

**Open Access** This article is licensed under a Creative Commons Attribution 4.0 International License, which permits use, sharing, adaptation, distribution and reproduction in any medium or format, as long as you give appropriate credit to the original author(s) and the source, provide a link to the Creative Commons licence, and indicate if changes were made. The images or other third party material in this article are included in the article’s Creative Commons licence, unless indicated otherwise in a credit line to the material. If material is not included in the article’s Creative Commons licence and your intended use is not permitted by statutory regulation or exceeds the permitted use, you will need to obtain permission directly from the copyright holder. To view a copy of this licence, visit <http://creativecommons.org/licenses/by/4.0/>.

© European Union, represented by The European Union and The Authors 2026

## Methods

### Computational framework

In this study, we consider four global warming levels that straddle a range from ambitious mitigation to virtually zero-emissions policies: from achieving the Paris Agreement goal of keeping the increase in global mean temperature to below 1.5 °C (relative to 1850–1900) or limiting it to 2 °C, to allowing it to reach 3 °C or even 4 °C. All global warming levels used in this study refer to increases in global mean temperature relative to the pre-industrial baseline (1850–1900)<sup>2</sup>. For each of these global warming levels, we generate probabilistic projections of extreme sea levels (ESLs, taken as relative sea level rise + storm surge levels + wave set-up + tides) that give rise to coastal flooding and combine them with exposure and vulnerability to quantify economic losses.

We define risk as a function of hazard, exposure and vulnerability, following the IPCC AR6 Risk Guideline<sup>45</sup>. As illustrated in the overall methodological framework in Supplementary Fig. 3, we integrated coastal flood maps for different ESL return periods under current (baseline) conditions and the above-mentioned global warming levels with road and rail segment information across Europe. Each road/rail segment is associated with maximum damage values, reflecting the total costs of reconstruction after a flood and DD curves that are specific to each different type of road and rail infrastructure. For each road/rail segment, and each type thereof, we calculated the corresponding damages for both high-return-period events (low-probability but high-impact events) and low-return-period events (high-probability but low-impact events), for ESLs up to the local coastal-protection level. The economic risk is expressed as the EAD, which is calculated as the area under the curve in a graph that plots the probability of ESL events against the resulting economic damage. Additionally, risk is here also quantified by the EALA, which represents the integration of flooded length of road/rail per ESL return period. More details on the different steps of the analysis are provided below.

### Hazard

We used coastal flood maps for different global warming levels as our hazard data. These maps were generated using the process-based two-dimensional hydraulic model LISFLOOD-ACC<sup>46,47</sup>, which is part of the LISFLOOD-FP model suite<sup>48</sup>. Following the methodology of Vousdoukas et al.<sup>49</sup>, we first computed ESLs at return periods of 1, 10, 20, 50, 100, 500 and 1,000 years (for the baseline and for the different warming levels) at 1-km spacing along the European coastline ('Exposure' section provides details). These ESLs were then used as input to LISFLOOD-ACC, together with proxy-based coastal flood protection levels, to produce flood maps consistent with the approach detailed in Vousdoukas et al.<sup>49</sup>

### Exposure

Our analysis covers 27 member-states of the European Union (that have a coastline, the UK, European Free Trade Association countries (excluding Iceland), and EU candidate countries (excluding Bosnia and Herzegovina). We also do not include overseas regions and territories of the above countries.

**Classification of road and rail networks.** In this study, we define surface transport infrastructure as comprising road and rail networks (that is linear assets), excluding other transport-related assets such as tunnels, bridges, ports and intermodal hubs. To simplify and harmonize the analysis, we first categorized the road and rail networks. For road types, we adopted the classification from Van Ginkel et al.<sup>27</sup>, which includes motorway, trunk, primary, secondary and tertiary roads. We used the OSM tagging convention as listed in Supplementary Table 7 to categorize them. For railways, we adopted three types: high-speed, conventional electrified and non-electrified. This classification is based on the significant differences in reconstruction costs depending on the train type and rail electrification arising from the different associated

technical specifications<sup>50</sup>. However, OSM data for the rail network is often insufficient for detailed classification<sup>51</sup>. To address this, we integrated information from the European Transport Policy Information System (ETIS) data<sup>52</sup>. We assigned ETIS data to OSM rail segments that were within 500 metres of ETIS rail segments and categorized them accordingly. OSM rail segments lacking data and not included in the ETIS network were assumed to be 'conventional non-electrified,' as ETIS data generally cover the major and more costly rail types, such as high-speed and electrified rails (Supplementary Table 7 provides more details).

**Maximum damage.** In quantitative risk assessment, maximum damage values per asset type are used together with flood depths to compute EADs. Here for road networks, we adopted Van Ginkel et al.'s<sup>27</sup> concept to determine the maximum damage for each road type and associated uncertainty, which is based on a review of original construction cost and reconstruction costs (that is, the cost of full or near-complete rebuilding of infrastructure, excluding land-acquisition costs, often restoring it to original standards after significant damage caused by a flood event) from road projects, primarily in Europe and a few from outside Europe. Roads with extra features such as street lights typically require more maintenance and incur higher damage costs after a flood. This is particularly true for motorways and trunk roads. Therefore, the maximum damage values were adjusted for these road types based on the presence or absence of street lights, by adopting corresponding higher or lower fractions of the construction cost, as shown in Supplementary Table 8. The uncertainty associated with flood velocity was also considered in determining the maximum damage to roads from floods. Low flood velocities generally result in minimal damage, whereas high flood velocities can cause severe damage<sup>53</sup>. To account for this uncertainty also, we adopted different fractions of the construction cost, depending on whether the flood velocity is low or high (Supplementary Table 8). Consequently, the maximum damage values for each road type (as given in Supplementary Table 8) consist of a range of reconstruction costs rather than a single fixed value to account for the uncertainty arising from variations in road construction costs and flood velocity.

For railways, the maximum damage estimates for different rail classes were derived from reconstruction costs provided by the REGIO Rail Unit Cost Tool, which reviewed 158 rail projects across Europe<sup>50</sup>. These costs are categorized into conventional non-electrified, conventional electrified and high-speed rails. For conventional non-electrified and electrified rails, the maximum damage is represented by the average reconstruction cost across all reviewed projects of the corresponding rail class, weighted by the rail length in each project (Supplementary Table 9). Reconstruction data for high-speed rail were limited; therefore, we estimated reconstruction costs by applying the average ratio of reconstruction to original construction costs reported for conventional electrified rail projects to the high-speed rail construction costs. The maximum damage for high-speed rails was then calculated as the length-weighted average of these reconstruction costs. To account for reconstruction cost variability for all rail types, based on the reported spread in costs, we set the maximum damage range from 50% higher to 50% lower than the estimated average reconstruction cost of new line construction costs across rail projects in the REGIO Unit Cost tool<sup>50</sup>. Although flood velocity can impact rail infrastructure, empirical data on flooding effects is currently unavailable. Therefore, we did not incorporate flood-velocity condition uncertainty into our rail damage calculations.

The maximum damage values across European countries are standardized by linearly scaling them using the average 2015 real gross domestic product (GDP) per capita of the former EU-28<sup>54</sup>. This standardization is necessary because the value of road and rail infrastructure per kilometre can vary significantly between countries due to their economic situation, including differences in labour costs, construction materials, subsoil conditions and so on.

## Vulnerability

The vulnerability of each road and rail type was quantified as a fraction of the maximum damage. This fraction was derived from the relationship between damage and flood depth, also known as the DD curve, for each ESL return period.

The DD curves for roads were adopted from Van Ginkel et al.<sup>27</sup>, which were developed through a detailed assessment of Europe-specific road types and the varying nature of road damage during floods. Van Ginkel et al.<sup>27</sup> developed a total of six DD curves (C1 to C6, as shown in Supplementary Fig. 4) based on road type, presence of road accessories and flood-velocity conditions. The DD curves appropriate for each road type and specific flood-velocity condition are detailed in Supplementary Table 10.

The DD curve for rail networks (RW, as shown in Supplementary Fig. 4) is derived from Bubeck et al.<sup>29</sup>, which is based on empirical evidence from a real flood event in Austria<sup>31</sup>. It should be noted that the reference case used to develop this DD curve for rail networks is a river flood with very low flood velocity. Similar to road infrastructure, flood velocity can influence the extent of rail damage. However, developing a rail damage curve for high-flood-velocity conditions is beyond the scope of this study due to the lack of empirical data and case studies (more details provided in the ‘Depth-Damage Curves’ section of the Supplementary Information).

## Risk

Here we performed our coastal flood-risk assessment in terms of EALA and EAD. To determine EALA, we calculated the potential flooded length of each road and rail segment for all return periods considered by intersecting the segment with the coastal flood extent for each ESL return period. The EALA for each segment was obtained by integrating these inundated lengths across all considered return periods.

Similarly, the EAD was calculated by integrating the damages (in monetary values) associated with the corresponding ESL return periods. These damage estimates for each road or rail segment were computed by multiplying the flooded length for a given return period, the damage fraction corresponding to the flooded depth (using appropriate DD curves as shown in Supplementary Fig. 4 and Supplementary Table 10) and the maximum damage value for the associated road or rail type (using Supplementary Tables 8 and 9). In the case of varying flood depths along the same road or rail segment, we used the average value as the representative flood depth for that segment. Because the maximum damage values for road and rail types comprise a range rather than a fixed value to account for uncertainty, the damage estimates also reflect this range. The damage for each segment is thus represented as a linearly scaled range, with minimum, 25%, 50%, 75% and maximum values of the range. (For example, if the estimated damage for a segment ranges from 100 to 1,000, it is represented as 100, 325, 550, 775 and 1,000, corresponding to the minimum, 25%, 50%, 75% and maximum values of the range.)

The EAD for each segment was calculated by integrating damages across all considered return periods, with results also represented as a linearly scaled range (minimum, 25%, 50%, 75% and maximum) to capture damage variability. We then report the EAD for each segment probabilistically using this scaled range. Two EAD values were selected per segment: one representing low-flood-velocity and one representing high-flood-velocity conditions. For example, for a rail segment, low-flood-velocity values were randomly selected from the lower portion of the range (minimum, 25% and 50%), whereas high-flood-velocity values were randomly drawn from the upper portion of the range (50%, 75% and maximum) (Supplementary Fig. 5 provides more details on this process for each road and rail type).

We then generated 1,000 EAD samples by assuming that the low- and high-flood-velocity EAD values correspond to  $-2$  and  $+2$  standard deviations, respectively, in a normal distribution (Supplementary Fig. 6). This process produces a probability

distribution of EAD for each segment. Further details on probabilistic EAD estimates can be found in the ‘Probabilistic EAD Estimates’ section of the Supplementary Information. The resulting EAD values are initially derived from standardized maximum damage estimates, based on the former EU-28 average 2015 GDP per capita. These EAD values are subsequently adjusted to reflect the local economic situation by reversing the standardization (by linearly rescaling from the former EU-28 average GDP per capita back to the national GDP per capita, while maintaining all values at 2015 euros).

These segment-level EAD distributions were subsequently aggregated at the NUTS3, NUTS0, IPCC AR6 subregion and European levels<sup>55,56</sup>. From the aggregated distribution at each spatial scale, the median EAD and its associated uncertainty range (5th–95th percentile) were extracted.

The EALAs and EADs thus computed at European and NUTS0 level are discussed in the manuscript. NUTS3 and IPCC AR6 subregion level results are presented in Supplementary Figs. 1 and 2 and Supplementary Tables 1 and 2.

## Comparison with previous studies

We compare our baseline EAD with estimates reported in previous studies on flood risk in Europe. For consistency, we limit our comparison to baseline estimates, as projections in these studies are reported for emissions scenarios, whereas ours are based on global warming levels. Our baseline estimates of €519 million (median value) are substantially lower than the €1.4 billion reported for coastal flood risk to all assets in Europe<sup>17</sup>. This difference is primarily due to the types of asset considered—our study focuses exclusively on surface transport infrastructure, whereas the previous estimate includes all 44 land-use classes from the refined CORINE land-use/land-cover dataset<sup>57</sup>. Additionally, variations in damage estimates arise from differences in methodology, such as the use of feature-based versus raster-based approaches, the selection of DD curves and the maximum damage values assigned to each asset type. Feature-based approaches, such as that employed in this study, are known to yield lower damage estimates than raster-based approaches<sup>27</sup>. Moreover, the shape of Huizinga et al.’s DD curve for transport infrastructure<sup>58</sup>, which is commonly used in raster-based approaches, probably results in higher damage estimates—particularly for lower flood depths—compared to the asset-specific DD curves for roads and rails used in our study.

We evaluated our baseline EAD for roads against a prior study on river flood risks<sup>27</sup> that employed the same feature-based approach, categories of roads, DD curves and maximum damage values adopted in our analysis. Our baseline EAD estimate of €188 million (median value) associated with coastal flood risk to road infrastructure is lower than the €230 million reported for river flood risks faced by roads. For rail infrastructure, we compared our results with a study on river flood damage<sup>29</sup>, where we adopted the same DD curves for rail types but used different, type-specific maximum damage values. Our estimate of €331 million (median value) for coastal flood rail damage is lower than the €581 million reported for river flood damage to rail networks.

As reported in the global multi-hazard risk assessment by Koks et al., damages from river floods are generally higher than those from coastal floods<sup>32</sup>. This difference is probably influenced by several factors. River floods often cover larger areas and occur more frequently due to extensive river networks and floodplains. Transport infrastructure and urban development along rivers typically extend over much longer distances than along coastlines, resulting in greater exposure to fluvial flooding than coastal flooding. Additionally, flood protection tends to be stronger and more consistent along coastlines, particularly in developed regions where coastal defences such as sea walls and surge barriers are common. In contrast, river flood defences are often less uniform and may be even insufficient in large basins or rapidly urbanizing regions. Therefore, the comparatively lower estimates for coastal flood risks in our study, relative to river flood risks, are not surprising.

## Limitations

The European-scale coastal flood risk to surface transport networks presented here for different global warming levels has a number of limitations that are unavoidable in a study of this scale. It is important that these limitations are borne in mind when interpreting our projections.

First, our analysis focused solely on road and rail networks, based on our definition of surface transport infrastructure, and excluded other transport-related infrastructure such as bus stops, train stations and intermodal hubs. We also did not include damage assessments for bridges and tunnels, as their flood damage mechanisms and assessment procedures differ fundamentally from those of regular roads and railways considered in this study.

For instance, bridge damage is typically caused by scour at foundations rather than surface inundation<sup>27,59–61</sup>, whereas tunnels are highly vulnerable to rapid flooding due to their underground positioning and typically limited drainage capacity<sup>62–64</sup>. Dewatering and restoration efforts in tunnels are logistically complex and resource intensive, potentially resulting in higher repair costs<sup>62–64</sup>. Most importantly, assessing flood damage in tunnels requires customized inundation modelling approaches that consider sub-catchments of floodwater, tunnel geometry, floodwater entry points and internal drainage systems to estimate the accumulated water depth within enclosed underground areas<sup>62,65</sup>. The coastal flood hazard data used in this study provide flood depths relative to ground level but do not include information on accumulated flood depths inside tunnels and therefore cannot be used to estimate tunnel-related flood damage. Intermodal hubs—ports, for example—contain a mix of infrastructure types and land uses, with damage mechanisms that can resemble those of buildings, transport networks, open areas or specialized facilities (for example, cranes), depending on their specific components and layout. These assets therefore require customized DD curves and maximum damage values (and customized flood modelling as well in the case of tunnels), which are not currently available in a comprehensive and harmonized form at the European scale. Therefore, we were unable to integrate them into our detailed risk assessment within the scope of this study. Their omission implies that our results do not capture the vulnerabilities or the complete risk across the entire transport sector.

Structural damage to these assets from coastal flooding could significantly increase total impacts, particularly where such infrastructures function as critical bottlenecks. We therefore encourage the development of Europe-specific vulnerability data for these transport infrastructure types and appropriate flood maps in the case of tunnels. Additionally, future work could investigate the indirect and cascading impacts resulting from the failure of road and rail networks, critical nodes such as intermodal hubs and stations and connections such as bridges and tunnels, which are very likely to further amplify the consequences of coastal flooding beyond the direct physical damages assessed in this study.

We excluded small islands less than one square kilometre in size, as neither global projections of most coastal flood drivers nor global DEMs are unlikely to be accurate for such small islands. The exposure data were sourced from community-contributed OSM, which may be incomplete in certain regions. Such incompleteness could affect the extent of exposure and potentially lead to underestimations in our EALA and EAD projections.

It is important to note that our analysis is based on existing transport networks, with no consideration of potential changes in exposure due to future socio-economic developments, or modifications in response to global warming, in the period 2020–2100. This is rather unlikely, as these networks will, in all probability, expand or retreat in response to socio-economic developments and global warming over this timeframe. Therefore, our impact and risk estimates are likely to be on the more conservative side. While incorporating plausible changes in exposure, particularly those aligned with Shared Socio-economic Pathways, would improve the robustness of our projections, no

dataset currently exists for Europe that captures both the spatial extent of future network changes and details on infrastructure type and functionality.

Such datasets could be developed by applying spatial modelling techniques—for example, by coupling future urban growth and land-use change models with transport network simulations to project where and how infrastructure might expand under different socio-economic and climate scenarios. When combined with other metrics, such as insights into how current infrastructure investments were made and which socio-economic indicators influenced those decisions, these approaches could enable the development of scenarios for future transport network expansion or retreat, albeit with a high level of inherent uncertainty<sup>66</sup>. We see this as a topic for future research, particularly for planning climate-resilient infrastructure systems at large spatial scales.

The DD curves used for road and rail infrastructure were originally developed for river flood-risk studies. However, different DD curves may be needed for coastal flooding of roads and railways, as coastal flooding involves additional factors such as wave action, wind and salinity, which can exacerbate damage<sup>67–70</sup>. Due to the lack of empirical evidence specific to transport infrastructure under coastal flood conditions, these additional impacts were not included in our current analysis.

Setiadji et al. found that submergence by salt-contaminated water causes a marginally larger impact of about 3% more damage to the uppermost asphalt layer of the roads<sup>71</sup>. However, saltwater can significantly increase rail degradation, especially by corrosion and result in higher maintenance costs<sup>72</sup>. Therefore, to partially account for this potential underestimation, we conducted a sensitivity analysis by shifting the depth thresholds defining the three damage classes in the rail DD curve towards lower values (Supplementary Fig. 7). This reflects the assumption that even shallower saltwater flooding may cause damage comparable to deeper freshwater flooding.

The results, presented in Supplementary Fig. 8, indicate that changes in the water depths for damage classes do lead to corresponding variations in the total EAD relating to rail. Specifically, for every 20% shift of the DD curve towards lower values of the water depth, for all corresponding damage classes, the total rail EAD increased by an average of 13%, indicating the rail EAD estimates are sensitive to assumptions regarding effects from coastal flood conditions. Whereas this sensitivity analysis provides a first-order indication of the potential influence of coastal-specific processes, such as salt-induced corrosion over time or wave-related mechanical damage, it still does not accurately represent real-world conditions. Coastal flood-specific DD curves (not available at present) that incorporate these processes based on empirical data would improve damage estimation for rail.

Coastal flood-specific DD curves could be developed based on empirical data such as detailed documentation from actual coastal flood events affecting road and rail infrastructure, preferably within the European context. This process should ideally include damage classification and validation of the newly developed DD curves or quantified parameters using simulated flood events and corresponding reported damages<sup>23,27</sup>. The development of such coastal flood-specific DD curves for road and rail infrastructure would enable a more accurate representation of vulnerability in coastal flood-risk assessments and projections. We therefore emphasize the need for further research aimed at gathering relevant empirical data and developing DD curves grounded in real-world coastal flood impacts on transport infrastructure.

## Data availability

Road and rail networks were extracted from OpenStreetMap data downloaded from <https://download.geofabrik.de/> (ref. 51). Additional information used to classify rail types was derived from the ETIS dataset, available at <https://www.tmleuven.be/en/project/etisplus> (ref. 52). DD curves and maximum damage values for road types

were taken from <https://doi.org/10.5194/nhess-21-1011-2021> (ref. 27), whereas DD curves for rail types were taken from <https://doi.org/10.1007/s10584-019-02434-5> (ref. 29). Estimates for maximum rail damage values were obtained using the REGIO Rail Unit Cost Tool developed by the European Commission, available at [https://ec.europa.eu/regional\\_policy/information-sources/publications/reports/2018/assessment-of-unit-costs-standard-prices-of-rail-projects-capital-expenditure\\_en](https://ec.europa.eu/regional_policy/information-sources/publications/reports/2018/assessment-of-unit-costs-standard-prices-of-rail-projects-capital-expenditure_en) (ref. 50). Low-elevation coastal zone data for each European country were sourced from <https://doi.org/10.7927/d1x1-d702> (ref. 38). Current transport volumes for road and rail networks in each European country are available via the European Commission's statistical pocketbook: [https://transport.ec.europa.eu/facts-funding/studies-data/eu-transport-figures-statistical-pocketbook/statistical-pocketbook-2024\\_en](https://transport.ec.europa.eu/facts-funding/studies-data/eu-transport-figures-statistical-pocketbook/statistical-pocketbook-2024_en) (ref. 41). National GDP at market prices in 2015 was downloaded from Eurostat: <https://doi.org/10.2908/TIPSAU10> (ref. 42), and annual government expenditure on surface transport infrastructure in each European country was obtained from <https://doi.org/10.2832/853267> (ref. 43). All data required to reproduce the figures in this study are available via Code Ocean at <https://doi.org/10.24433/CO.9918929.v1> (ref. 73).

## Code availability

Python scripts developed for the analysis are available via Code Ocean at <https://doi.org/10.24433/CO.9918929.v1> (ref. 73).

## References

45. IPCC in *Climate Change 2014: Synthesis Report* (eds Core Writing Team et al.) 151 (IPCC, 2014).
46. Bates, P. D., Horritt, M. S. & Fewtrell, T. J. A simple inertial formulation of the shallow water equations for efficient two-dimensional flood inundation modelling. *J. Hydrol.* **387**, 33–45 (2010).
47. Neal, J. C. et al. Evaluating a new LISFLOOD FP formulation with data from the summer 2007 floods in Tewkesbury, UK. *J. Flood Risk Manage.* **4**, 88–95 (2011).
48. Bates, P. D. & De Roo, A. P. J. A simple raster-based model for flood inundation simulation. *J. Hydrol.* **236**, 54–77 (2000).
49. Vousdoukas, M. I. et al. Small island developing states under threat by rising seas even in a 1.5 °C warming world. *Nat. Sustain.* **6**, 1552–1564 (2023).
50. Attinà, M. et al. *Assessment of Unit Costs (Standard Prices) of Rail Projects (CAPital Expenditure)* (Publications Office of the European Union, 2018).
51. OpenStreetMap contributors. *Planet Dump* (OpenStreetMap Foundation, 2024); <https://planet.openstreetmap.org>
52. ETISplus Consortium *European Transport Policy Information System Plus (ETISplus) Database* (European Commission, DG MOVE, Panteia/NEA, 2012); <https://www.tmluven.be/en/project/etisplus>
53. Kreibich, H. et al. Is flow velocity a significant parameter in flood damage modelling? *Nat. Hazards Earth Syst. Sci.* **9**, 1679–1692 (2009).
54. Eurostat *Real GDP Per Capita* (Statistical Office of the European Union, European Commission, 2021); [https://doi.org/10.2908/SDG\\_08\\_10](https://doi.org/10.2908/SDG_08_10)
55. *EuroRegionalMap* (EuroGeographics, accessed 11 November 2025); <https://www.mapsforeurope.org/explore-map/euro-regional-map>
56. Iturbide, M. et al. Repository supporting the implementation of FAIR principles in the IPCC-WG1 Atlas. *Zenodo* <https://doi.org/10.5281/zenodo.5171760> (2021).
57. Batista e Silva, F., Lavalle, C. & Koomen, E. A procedure to obtain a refined European land use/cover map. *J. Land Use Sci.* **8**, 255–283 (2013).
58. Huizinga, J. *Flood Damage Functions for EU Member States* (HKV Consultants, 2007).
59. Lamb, R., Garside, P., Pant, R. & Hall, J. W. A probabilistic model of the economic risk to Britain's railway network from bridge scour during floods. *Risk Anal.* **39**, 2457–2478 (2019).
60. Pregnolato, M. Bridge safety is not for granted—a novel approach to bridge management. *Eng. Struct.* **196**, 109193 (2019).
61. Vennapus, P. K. R., White, D. J. & Miller, D. K. *Western Iowa Missouri River Flooding—Geo-Infrastructure Damage Assessment, Repair and Mitigation Strategies* InTrans Project Reports 97, 180 (Iowa State University, 2013).
62. Yuan, X., Wu, M., Tian, F., Wang, X. & Wang, R. Identification of influencing factors and risk assessment of underground space flooding in the mountain city. *Int. J. Disaster Risk Reduct.* **113**, 104807 (2024).
63. Forero-Ortiz, E., Martínez-Gomariz, E., Cañas Porcuna, M., Locatelli, L. & Russo, B. Flood risk assessment in an underground railway system under the impact of climate change—a case study of the Barcelona metro. *Sustainability* **12**, 5291 (2020).
64. Huang, H., Zhang, D. & Huang, Z. Resilience of city underground infrastructure under multi-hazards impact: from structural level to network level. *Resilient Cities Struct.* **1**, 76–86 (2022).
65. Lyu, H. M., Shen, S. L., Yang, J. & Yin, Z. Y. Inundation analysis of metro systems with the storm water management model incorporated into a geographical information system: a case study in Shanghai. *Hydrol. Earth Syst. Sci.* **23**, 4293–4307 (2019).
66. Dellink, R., Chateau, J., Lanzi, E. & Magné, B. Long-term economic growth projections in the Shared Socioeconomic Pathways. *Glob. Environ. Change* **42**, 200–214 (2017).
67. Bates, P. D. et al. Combined modeling of US fluvial, pluvial, and coastal flood hazard under current and future climates. *Water Resour. Res.* **57**, e2020WRO28673 (2021).
68. Argyroudis, S., Mitoulis, S., Winter, M. & Kaynia, A. Fragility of transport assets exposed to multiple hazards: state-of-the-art review toward infrastructural resilience. *Reliab. Eng. Syst. Saf.* **191**, 106567 (2019).
69. Valdez, B. et al. Corrosion assessment of infrastructure assets in coastal seas. *J. Mar. Eng. Technol.* **15**, 124–134 (2016).
70. Zimmerman, R. & Faris, C. Chapter 4: infrastructure impacts and adaptation challenges. *Ann. N.Y. Acad. Sci.* **1196**, 63–86 (2010).
71. Setiadji, B. H., Utomo, S. & Nahyo Effect of chemical compounds in tidal water on asphalt pavement mixture. *Int. J. Pavement Res. Technol.* **10**, 122–130 (2017).
72. Xu, W. et al. Corrosion of rail tracks and their protection. *Corros. Rev.* **39**, 1–13 (2021).
73. Nawarat, K. Global warming-induced coastal flood risk to European surface transport infrastructure. *Code Ocean* <https://doi.org/10.24433/CO.9918929.v1> (2025).

## Acknowledgements

This research is funded by the AXA Research Fund and IHE Delft's Water and Development Partnership Program (WDPP). K.v.G. acknowledges funding from the Horizon-Europe ACCREU Project, grant agreement number 101081358. We would also like to acknowledge OpenStreetMap contributors for the map data available at <https://www.openstreetmap.org>. Administrative boundaries for figures (NUTS 0/3) are derived from EuroGeographics' EuroRegionalMap (version 2025). This dataset includes Intellectual Property from European National Mapping and Cadastral Authorities and is licenced on behalf of these by EuroGeographics. The original dataset is available for free at <https://www.mapsforeurope.org>, with licence terms at <https://www.mapsforeurope.org/licence>. All attribution statements can be found at <https://www.mapsforeurope.org/attributions>.

## Author contributions

K.N., J.R., R.R., M.I.V. and L.F. conceived the study. M.I.V. produced the coastal flood maps by global warming levels. E.M. contributed to

defining the maximum damage value for rail infrastructure. K.N., J.R. and R.R. contributed to refining the methodology. K.N. performed the analysis, prepared the figures and wrote the original draft. K.N., R.R. and J.R. contributed to subsequent revisions. All authors (K.N., J.R., R.R., M.I.V., L.F, K.v.G. and E.M.) contributed to editing and improving the manuscript.

### Competing interests

The authors declare no competing interests.

### Additional information

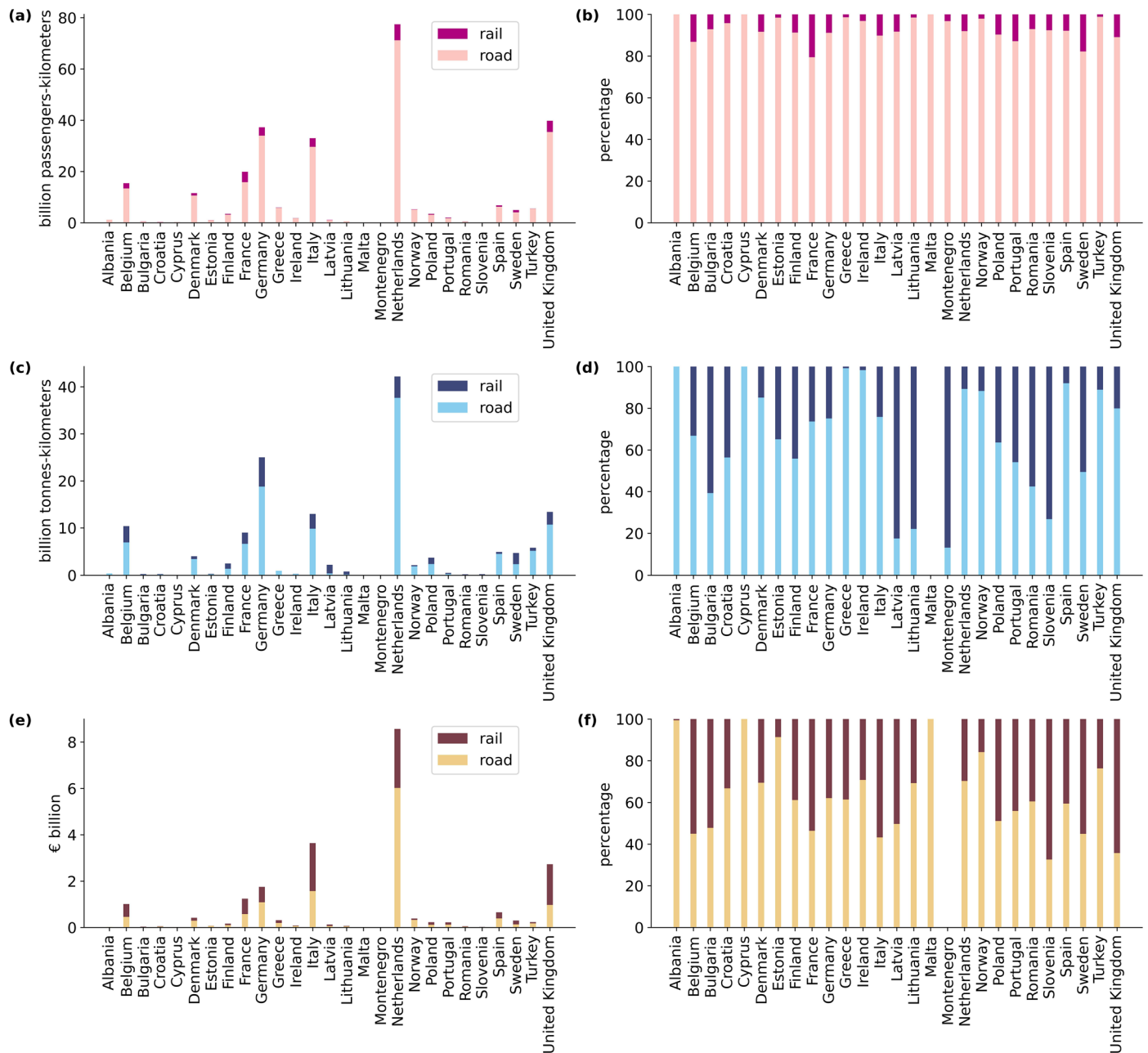
**Extended data** is available for this paper at <https://doi.org/10.1038/s41558-025-02510-y>.

**Supplementary information** The online version contains supplementary material available at <https://doi.org/10.1038/s41558-025-02510-y>.

**Correspondence and requests for materials** should be addressed to Khin Nawarat or Luc Feyen.

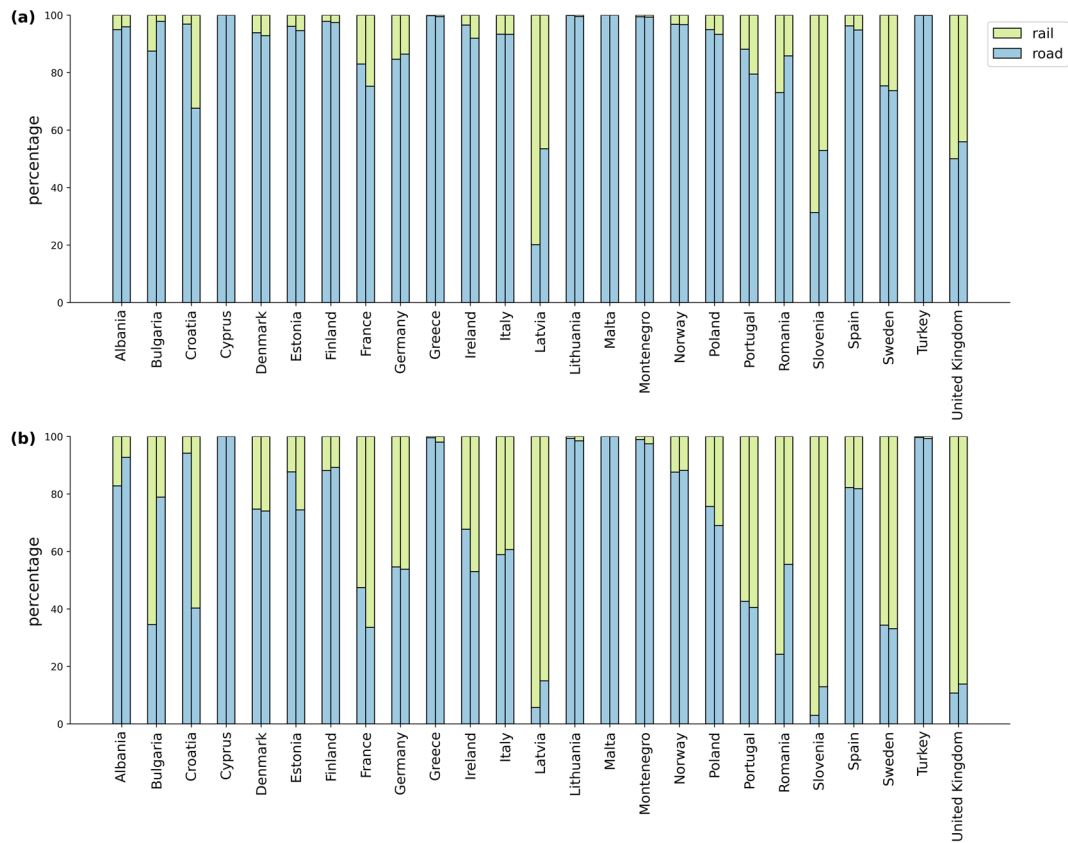
**Peer review information** *Nature Climate Change* thanks Ellena Marta, Michelle Ochsner and the other, anonymous, reviewer(s) for their contribution to the peer review of this work.

**Reprints and permissions information** is available at [www.nature.com/reprints](http://www.nature.com/reprints).



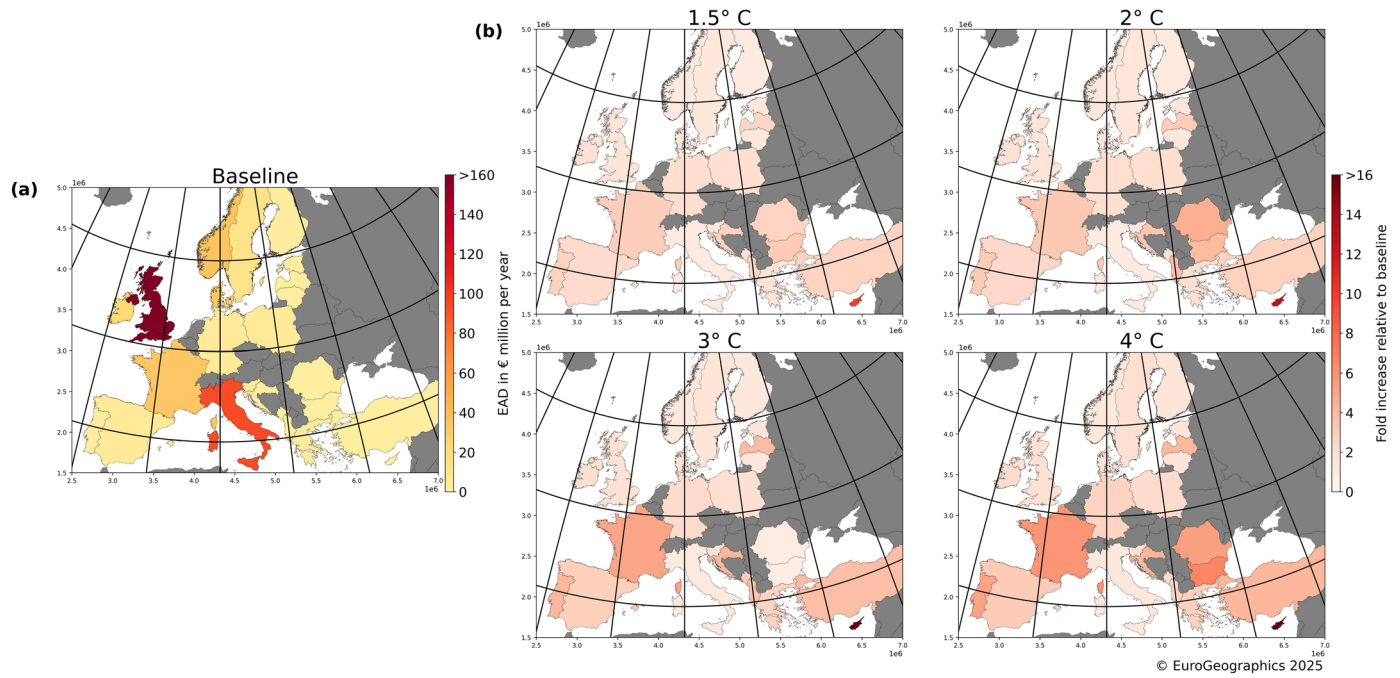
**Extended Data Fig. 1 | Current transport volume and annual government expenditure on surface transport infrastructure in Europe. (a)** Passenger transport volume in low-elevation coastal zone (LECZ), **(b)** Shares of road and rail network usage for total passenger transport volume, **(c)** Haulage transport volume in LECZ, **(d)** Shares of road and rail network usage for total haulage transport volume (values for Malta is negligible), **(e)** Annual government expenditure on transport infrastructure in LECZ (Data for Montenegro is not

available), and **(f)** Shares of total annual government expenditure on road and rail networks (Data for Montenegro is not available). [Data sources: European Commission: Directorate-General for Mobility and Transport, EU Transport in Figures: Statistical Pocketbook (2024) and Overview of transport infrastructure expenditures and costs, European Commission: Directorate-General for Mobility Transport (2019)].



**Extended Data Fig. 2 | Relative contributions of road and rail associated flood risk to total coastal flood risk in Europe for baseline conditions and for 2 °C of global warming. (a) Relative contributions of road and rail to the total expected**

annual length affected (EALA), and (b) Relative contributions of road and rail to the total expected annual damage (EAD). (Stacked bars are arranged sequentially from left to right for the baseline condition and the 2 °C global warming level.).



**Extended Data Fig. 3 | Coastal flood risk to surface transport infrastructure in Europe expressed as expected annual damage (EAD) for different global warming levels at country scale. (a)** Baseline EAD (the estimate under 1980–2020 climate conditions), and **(b)** Projected change in EAD from the baseline value for different global warming levels. The Netherlands and Belgium are not

affected by the range of flood-return periods considered in this study due to their high levels of coastal protection. Basemap administrative boundaries from EuroGeographics 2025 under a licence available at <https://www.mapsforeurope.org/licence>.